Differential electronic-excitation cross sections of molecular oxygen by electron impact: The $a\ ^1\Delta_g$ and $b\ ^1\Sigma_g$ states

Tong W. Shyn and Christopher J. Sweeney
Space Physics Research Laboratory, University of Michigan, Ann Arbor, Michigan 48109-2143
(Received 28 September 1992)

We have measured the differential excitation cross sections of the $a\ ^1\Delta_g$ and $b\ ^1\Sigma_g$ states of molecular oxygen by electron impact. The energy range was from 5.0 to 20 eV. The angular range was from 12° to 156°. We found maximum cross sections near 7 eV for the electronic excitations. Our results are compared with theory and other experimental results. Our results agree very well with theoretical prediction at 5 eV, but other experimental results have noteworthy differences.

PACS number(s): 34.80.Gs

I. INTRODUCTION

Total scattering cross sections and elastic cross sections of molecular oxygen have been measured by a number of investigators, but only a few fragmentary measurements on the electronic excitation cross sections of the $a\ ^1\Delta_g$ and $b\ ^1\Sigma_g$ states are available. Trajmar *et al.* [1] measured the excitation cross sections for the energy range 4–45 eV and scattering angles 10°–90°. Linder and Schmidt [2] have measured the $a\ ^1\Delta_g$ excitation cross sections for the energy range 1.5–4.0 eV, and Wakiya [3] has measured the cross sections above 20 eV impact energy.

Chang [4] obtained the relative angular distributions of electrons excited to the $a\ ^1\Delta_g$ and $b\ ^1\Sigma_g$ states at 4.5 eV impact energy using the frame-transformation theory. Agreement with the measurements of Trajmar *et al.* is very good with respect to angular shape.

Noble and Burke [5] calculated the integrated excitation cross sections of the $a\ ^1\Delta_g$ and $b\ ^1\Sigma_g$ states for the energy range from threshold to 20 eV using the R-matrix method.

This paper presents experimental results of differential excitation cross sections of the $a\ ^1\Delta_g$ and $b\ ^1\Sigma_g$ states of molecular oxygen measured by a crossed-beam method. The energy and angular ranges measured were 5–20 eV and 12°–156°, respectively.

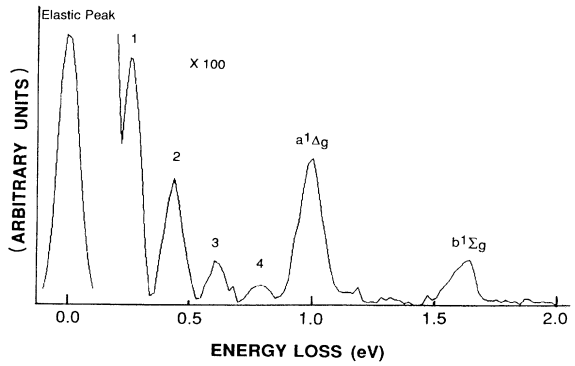

FIG. 1. Energy-loss spectrum of O_2 at 84° and 7 eV impact energy.

II. APPARATUS AND PROCEDURE

A schematic diagram of the apparatus for the present measurements is the same as for the measurement of the vibrational excitation cross sections of CH_4 and H_2O published previously [6,7]. Briefly, differentially pumped upper and lower changers contain the apparatus. A neutral-O_2-beam source is located in the upper chamber. The vertically collimated O_2 beam from the source enters the lower chamber through a double skimmer located between the two chambers. The monoenergetic-electron-beam source and an electron-energy-analyzer system (in the horizontal plane) are located in the lower chamber.

The electron-beam source consists of an electron gun, a 127° energy selector, two electron lenses, and two electron-beam deflectors. It is rotatable from −90° to +160° continuously. During the present set of measurements, the electron source produces an electron current of 10^{-9} A with an energy resolution of 80 meV full width

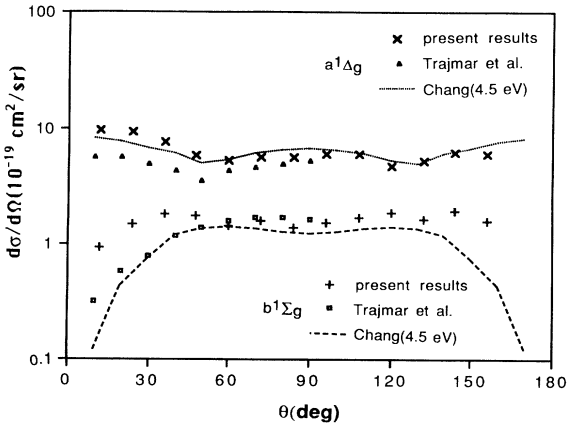

FIG. 2. Differential excitation cross section of the $a\ ^1\Delta_g$ and $b\ ^1\Sigma_g$ states at 5 eV impact energy, along with the results of Trajmar *et al.* [1] and the theoretical results of Chang [4].

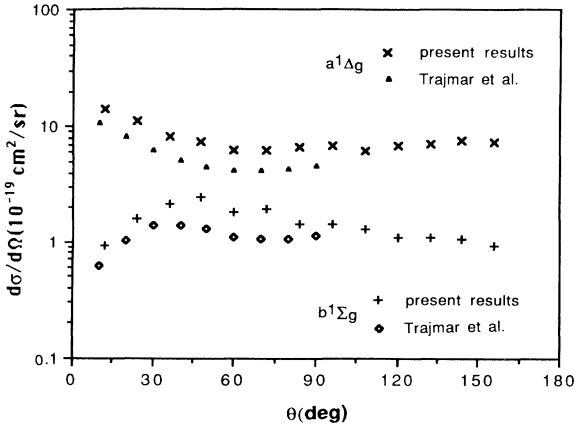

FIG. 3. Differential excitation cross section of the $a\ ^1\Delta_g$ and $b\ ^1\Sigma_g$ states at 10 eV impact energy, along with the results of Trajmar *et al.* [1].

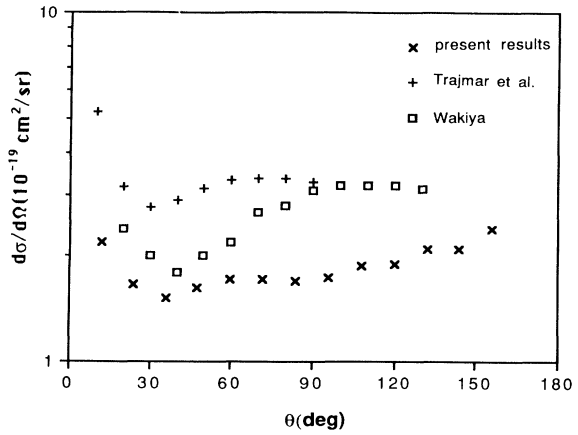

FIG. 4. Differential excitation cross section of the $a\ ^1\Delta_g$ state at 20 eV impact energy, along with the results of Trajmar *et al.* [1] and of Wakiya [3].

at half maximum at 5 eV incident energy, and better resolution for higher energies. Our fixed-detector system consists of two electrostatic energy analyzers placed in series, two electron lenses, and a channeltron electron multiplier. This double-analyzer system has an energy resolution of better than 60 meV and reduces the background signal compared to our previously used single-analyzer system by a factor of approximately 100. The solid angle of detection is about 5×10^{-4} sr. The divergence angle of the incident electron beam is $\pm3°$.

The incident-electron beam of a given energy intersects the collimated neutral beam in the interaction region. The scattered electrons from the O_2 beam at a given angle are detected by the electron channeltron multiplier after energy analysis. Thus, the energy-loss spectrum of the scattered electrons is obtained at a given scattering angle and incident energy. This procedure is repeated for different angles and incident energies. A typical energy-loss spectrum at 84° with 7 eV impact electron energy is shown in Fig. 1. The elastic peak is shown. The $a\ ^1\Delta_g$ and $b\ ^1\Sigma_g$ states are well defined and there are also four vibrational states (denoted 1–4) between the elastic peak and the $a\ ^1\Delta_g$ state. The energy resolution of the present apparatus is not sufficient to resolve the rotational excitations. The absolute excitation cross section at a given angle is obtained by normalizing against the absolute elastic cross sections of O_2, which were measured by the present author [8].

The impact energy scale is calibrated against the 19.3-eV resonance of He. Three sets of Helmholtz coils reduce stray magnetic fields down to less than 20 mG in all directions near the interaction region.

III. EXPERIMENTAL RESULTS

We measured the differential excitation cross sections for the $a\ ^1\Delta_g$ and $b\ ^1\Sigma_g$ states at incident energies of 5.0, 7.0, 10, 15, and 20 eV. The final results are shown in

TABLE I. Differential electronic excitation cross sections of O_2 for (a) $a\ ^1\Delta_g$ and (b) $b\ ^1\Sigma_g$ states. Numbers in parentheses are extrapolated data points.

	θ (deg)														
E (eV)	12	24	36	48	60	72	84	96	108	120	132	144	156	168	σ_i (10^{-18} cm^2)
							(a) $d\sigma(a\ ^1\Delta_g)/d\Omega(10^{-19}\,\mathrm{cm}^2/\mathrm{sr})$								
5.0	9.9	9.5	7.8	5.8	5.3	5.7	5.7	6.2	6.1	4.9	5.3	6.3	6.1	(6.1)	7.6
7.0	12.3	11	9.3	6.9	5.8	6.4	6.5	7.4	7.9	8.6	9.9	11	12	(12)	10.4
10	14	11	8.2	7.4	6.3	6.2	6.7	7.0	6.3	6.9	7.2	7.6	7.6	(7.7)	7.7
15	4.4	2.9	2.7	2.4	2.7	2.9	2.8	3.2	3.5	3.7	4.2	4.3	4.8	(4.9)	4.2
20	2.2	1.7	1.5	1.6	1.7	1.7	1.7	1.7	1.9	1.9	2.1	2.1	2.4	(2.5)	2.3
							(b) $d\sigma(b\ ^1\Sigma_g)/d\Omega$ ($10^{-20}\,\mathrm{cm}^2/\mathrm{sr}$)								
5.0	9.4	15	18	17	14	16	14	15	17	19	16	19	16	(11)	2.0
7.0	8.8	23	29	31	28	27	29	26	27	30	27	25	20	(13)	3.3
10	9.3	16	21	24	18	19	14	14	13	11	11	11	9.1	(7.3)	1.9
15	3.9	8.5	8.9	10	7.9	7.4	6.2	5.5	5.3	4.5	4.7	3.5	3.1	(2.4)	0.78
20	2.6	4.7	6.0	6.1	5.8	5.7	5.5	5.0	4.2	3.3	2.5	1.8	0.9	(0.5)	0.55

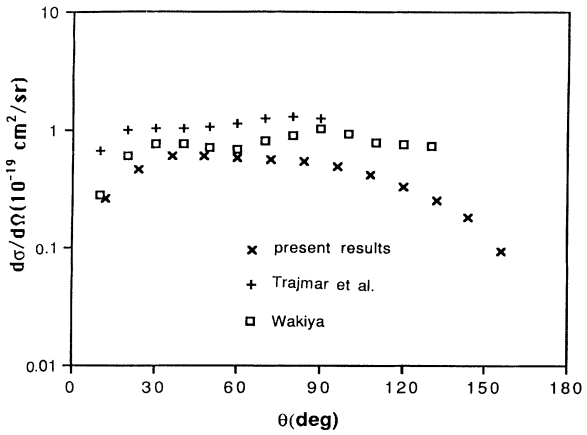

FIG. 5. Differential excitation cross section of the $b\ ^1\Sigma_g$ state at 20 eV impact energy, along with the results of Trajmar *et al.* [1] and of Wakiya [3].

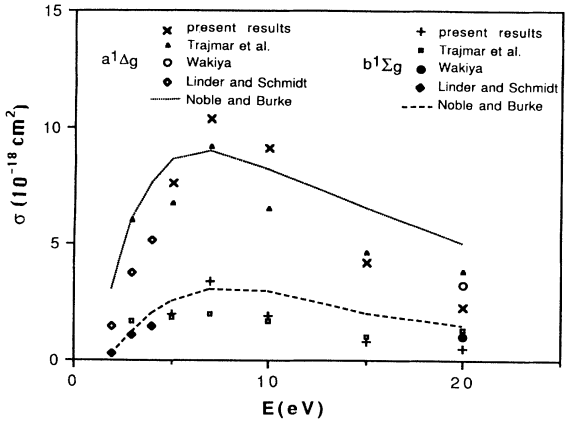

FIG. 6. Integrated excitation cross sections of the $a\ ^1\Delta_g$ and $b\ ^1\Sigma_g$ states, along with the experimental results of Trajmar *et al.* [1], Wakiya [3], and Linder and Schmidt [2], and the theoretical results of Noble and Burke [5].

Table I.

The statistical uncertainty of the data points is less than ±6% for the $a\ ^1\Delta_g$ and ±8% for the $b\ ^1\Sigma_g$ state. The uncertainty in the transmission efficiency of the detector due to the electron-lens effects is ±5%. The overall uncertainty of the present results is ±16% for the $a\ ^1\Delta_g$ state and ±18% for the $b\ ^1\Sigma_g$ state, including the uncertainty in the O_2 elastic cross sections (±14%).

Figure 2 shows the differential excitation cross sections of the $a\ ^1\Delta_g$ and $b\ ^1\Sigma_g$ states at 5 eV, along with those of Trajmar *et al.* and the theoretical results of Chang, whose results were normalized to the present results at 60°. The results of Trajmar *et al.* agree relatively well with the present results, except at extreme forward directions, where their results for both states are smaller than ours by a factor of approximately 2. Two local minima can be seen near 60° and 120°; this is consistent with Chang's predictions. The angular distributions of 7 and 15 eV impact have a similar trend as those of 5 eV impact.

Figure 3 is the same as Fig. 2, except for 10 eV impact. Agreement between the two measurements is very good with respect to angular shape for both states, but the magnitudes reported by Trajmar *et al.* are smaller than the present results by about 30%.

Figure 4 shows different excitation cross sections of the $a\ ^1\Delta_g$ state at 20 eV impact, along with the results of Trajmar *et al.* and those of Wakiya. The shape of the results of Trajmar *et al.* agrees very well with that of the present results; however, the magnitudes of the cross sections are larger than the present results by about a factor of 2. The results of Wakiya agree with the present results from 30° to 60° within the uncertainty, but his values are larger than the present results below 30° and above 60° by about a factor of 2. Figure 5 is the same as Fig. 4, except for the $b\ ^1\Sigma_g$ state. The two previous measurements show a trend similar to that of the $a\ ^1\Delta_g$ state.

Finally, Fig. 6 shows integrated cross sections of the $a\ ^1\Delta_g$ and $b\ ^1\Sigma_g$ states, along with the results of Linder and Schmidt, of Trajmar *et al.*, Wakiya, and also the theoretical results of Noble and Burke. The present results have larger values for the $a\ ^1\Delta_g$ state than those of Trajmar *et al.* This may be due to the large angular region for extrapolations—from 90° to 180°. For the $b\ ^1\Sigma_g$ state, relatively good agreement exists, except for 7 eV impact energy. The present result is larger than those of Trajmar *et al.*, by about 40%. Wakiya's results at 20 eV are larger than the present results for both the $a\ ^1\Delta_g$ and $b\ ^1\Sigma_g$ states by about 30%. The results of Linder and Schmidt have trends that are consistent with the present results. The theoretical results of Noble and Burke have larger values below 5 and above 15 eV, and smaller values between 5 and 10 eV.

ACKNOWLEDGMENT

This work was supported by the U. S. National Science Foundation under Grant No. ATM-9020626.

[1] S. Trajmar, D. C. Cartwright, and W. Williams, Phys. Rev. A **4**, 1482 (1971).
[2] F. Linder and H. Scmidt, Z. Naturforsch. **26**, 1617 (1971).
[3] K. Wakiya, J. Phys. B **11**, 3931 (1978).
[4] E. S. Chang, J. Phys. B **10**, L677 (1977).
[5] C. J. Noble and P. G. Burke, J. Phys. B **19**, L35 (1986).
[6] T. W. Shyn and T. E. Cravens, J. Phys. B **23**, 293 (1990).
[7] T. W. Shyn, S. Y. Cho, and T. E. Cravens, Phys. Rev. A **38**, 678 (1988).
[8] T. W. Shyn and W. E. Sharp, Phys. Rev. A **26**, 1369 (1982).